Noise Elimination of a Multi-tone Broadband Noise with Hybrid Helmholtz Mufflers Using a Simulated Annealing Method

Min-Chie CHIU

Department of Mechanical and Automation Engineering, Chung Chou University of Science and Technology
No. 6, Lane 2, Sec.3, Shanchiao Rd., Yuanlin, Changhua 51003, Taiwan, R.O.C.; e-mail: minchie.chiu@msa.hinet.net

Noise control is essential in an enclosed machine room where the noise level has to comply with the occupational safety and health act. In order to overcome a pure tone noise with a high peak value that is harmful to human hearing, a traditional reactive muffler has been used. However, the traditional method for designing a reactive muffler has proven to be time-consuming and insufficient. In order to efficiently reduce the peak noise level, interest in shape optimization of a Helmholtz muffler is coming to the forefront.

Helmholtz mufflers that deal with a pure tone have been adequately researched. However, the shape optimization of multi-chamber Helmholtz mufflers that deal with a broadband noise hybridized with multiple tones within a constrained space has been mostly ignored. Therefore, this study analyzes the sound transmission loss (STL) and the best optimized design for a hybrid Helmholtz muffler under a space-constrained situation. On the basis of the plane wave theory, the four-pole system matrix used to evaluate the acoustic performance of a multi-tone hybrid Helmholtz muffler is presented. Two numerical cases for eliminating one/two tone noises emitted from a machine room using six kinds of mufflers (muffler A∼F) is also introduced. To find the best acoustical performance of a space-constrained muffler, a numerical assessment using a simulated annealing (SA) method is adopted. Before the SA operation can be carried out, the accuracy of the mathematical model has been checked using the experimental data. Eliminating a broadband noise hybridized with a pure tone (130 Hz) in Case I reveals that muffler C composed of a one-chamber Helmholtz Resonator and a one-chamber dissipative element has a noise reduction of 54.9 (dB). Moreover, as indicated in Case II, muffler F, a two-chamber Helmholtz Resonator and a one-chamber dissipative element, has a noise reduction of 69.7 (dB). Obviously, the peak values of the pure tones in Case I and Case II are efficiently reduced after the muffler is added.

Consequently, a successful approach in eliminating a broadband noise hybridized with multiple tones using optimally shaped hybrid Helmholtz mufflers and a simulated annealing method within a constrained space is demonstrated.

Keywords: multiple tones, hybrid, Helmholtz, four-pole transfer matrix method, SA method.

Notations

c_o – sound speed (m s^{-1}),

$C_{\rm res}$ – the acoustic compliance $\left(= \dfrac{V_c}{\rho_o c_o^2}\right)$,

DD, DD_1 – diameter of the inner tubes (m),

D_o – diameter of the outer chamber (m),

f – cyclic frequency (Hz),

dH – the diameter of a perforated hole on the perforated tube (m),

HR – Helmholtz Resonator,

iter – maximum iteration in SA,

k_o – wave number $\left(= \dfrac{\omega}{c_o}\right)$,

kk – cooling rate in SA,

L_o – total length of the muffler (m),

L_k – the length of the resonating neck (m),

$L_{\rm res}$ – the acoustic inertia $\left(= \dfrac{\rho_o(L_k + \ell_T)}{S_k}\right)$,

ℓ_T – the total end correction $(= \ell_1 + \ell_2 = 1.698 r_k)$ (m),

OBJ – objective function (dB),

p – acoustic pressure (Pa),

$p\%$ – the porosity of the perforated tube in the dissipative element,

Q – volume flow rate of venting gas (m^3 s^{-1}),

r_k – the radius of the resonating tube in the Helmholtz resonator (m),

$R_{\rm res}$ – the acoustic resistance,

SA – simulated annealing,

S_i – the section area at the i-th node (m^2),

S_d – the section area of the main duct connected to the Helmholtz resonator (m^2),

S_k – the section area of the resonating tube in the Helmholtz resonator (m^2),

STL – sound transmission loss (dB),

SWL_T – overall sound power level inside the muffler's output (dB),

T^*_{ij} – components of a four-pole transfer system matrix,

$TS_{ij}, TSC_{ij}, TSE_{ij}, THR_{ij}$ – components of four-pole transfer matrices for an acoustical mechanism with a straight duct, a sudden contraction element, a sudden expansion element, and a Helmholtz resonator,

u – acoustic particle velocity ($m\ s^{-1}$),

ν – acoustic mass velocity ($kg\ s^{-1}$),

Z_r – acoustical impedance of the Helmholtz resonator $\left(= \dfrac{p_2}{\rho_o S_2 u_2}\right)$,

ρ_o – air density ($kg\ m^{-3}$),

σ_{fr} – the acoustical flowing resistance for the wool (rayls/m),

ω – angular velocity ($= 2\pi f$),

V_c – the volume of the resonator (m^3).

1. Introduction

As pointed out by the Occupational Safety and Health Act (OSHA) of 1970, high pure tone noise levels can be harmful to workers and can not only lead to psychological but also to physiological ailments. Consequently, noise control work on equipment becomes vital (CHEREMISINOFF, 1977; ALLEY *et al.*, 1989). LEUG (1936) and OLSON & MAY (1953) started the study of noise control for a low frequency noise in 1936 and 1953. HELMHOLTZ (1877) and RAYLEIGH (1896) proposed a design for noise reduction using a Helmholtz Resonator (*HR*) with an opening. An *HR*, which is analogous to an acoustical filter connected with a small open-top tube used to tune a specified frequency (LORD, RAYLEIGH, 1945; INGARD, 1953), is a certain passive acoustical element widely used in aircraft cabins, dining cars, and a ship's engine room. To accurately predict the resonant frequency of the *HR*, a series of studies has been developed. INGARD (1953) investigated the end correction for various openings of the *HR*. Considering the motion effect within an empty chamber, ALSTER (1972) proposed an improved model for the end correction that is related to the shape of the chamber. CHANAUD (1994) extended the study of IN-GARD (1953) for a large-size chamber; moreover, he analyzed the influence of the resonant frequency with respect to the location of the opening. SUGIMOTO (1992) and HORIOKA (1995) proposed a new design by adding a matrix type *HR* within a channel. Additionally, they utilized shape optimization for a specified tone without space limitations. CUMMINGS (1992), DORIA (1995), FAHY & SCHOFIELD (1980), and LI & CHENG (2007) successfully assessed the resonant frequency for an enclosure that was composed of the *HR* device. DICKEY and SELAMET (1996) analyzed the resonant frequency of a non-symmetric chamber using a three-dimensional boundary element method. CHANAUD (1997) assessed the influence of the resonant frequency with respect to various locations of a resonating tube; additionally,

he studied the influence of the resonant frequency for a rectangular chamber with a square opening. HSIEH (2003) assessed the acoustical performance of a motorcycle composed of a wool/non-wool *HR* silencer using a four-pole matrix and a boundary element method. TANG (2005) investigated the influence of the resonant frequency with respect to a cone-type resonating tube.

In practical engineering work, the constrained problem is mostly concerned with the necessity of operation and maintenance where there is a growing need to optimize the acoustical performance within a confined space. Moreover, a broadband noise hybridized with multiple tones that will lead to psychological and physiological ailments becomes essential. However, in the above research, the assessment in finding a muffler's optimal shape design for a broadband noise hybridized with multiple tones within a constrained space has been somewhat neglected. In order to promote the best acoustical performance in mufflers, three kinds of hybrid two-chamber mufflers (muffler A: a one-chamber *HR* element and a one-chamber simple expansion element; muffler B: a one-chamber *HR* element and a one-chamber tube-extended element; muffler C: a one-chamber *HR* element and a one-chamber dissipative element) used in eliminating a broadband noise hybridized with one tone will be proposed. Also, in order to reduce a broadband noise hybridized with two tones, three kinds of hybrid three-chamber mufflers (muffler D: a two-chamber *HR* element and a one-chamber simple expansion element; muffler E: a two-chamber *HR* element and a one-chamber tube-extended element; muffler F: a two-chamber *HR* element and a one-chamber dissipative element) within a fixed space are also presented. To facilitate the numerical assessment, two different *SA* techniques (a cooling rate and an iteration) are adopted. By adjusting the muffler's shape, varying the acoustical element, and using the *SA*, the optimal acoustical performance of the mufflers can be achieved.

2. Theoretical background

As illustrated in Fig. 1, there is a broadband noise hybridized with multiple tones in the constrained ma-
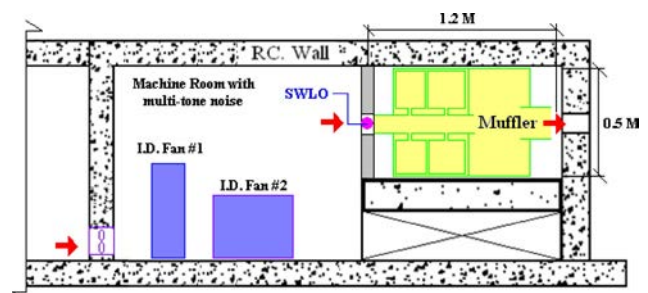

Fig. 1. A confined machine room with multiple tones.

chine room. The three kinds of mufflers A∼C shown in Fig. 2 were adopted in dealing with a broadband noise hybridized with one tone (130 Hz). Moreover, three kinds of mufflers (muffler D∼F) shown in Fig. 3 were
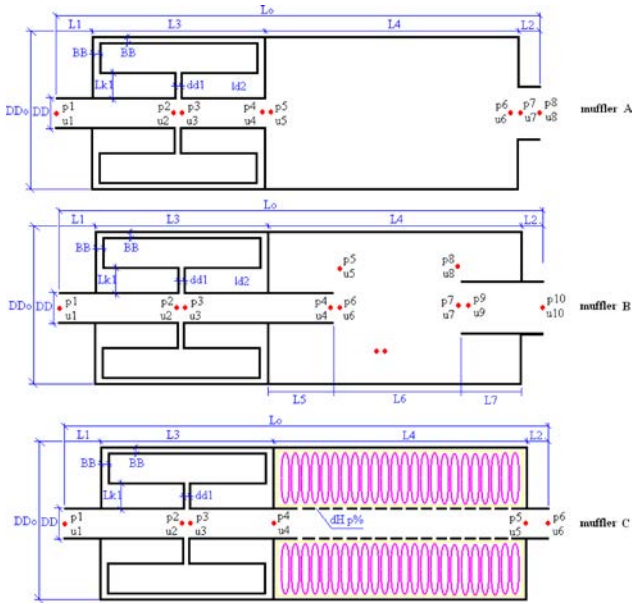

Fig. 2. The dimension and acoustical nodes for three kinds of one-chamber Helmholtz mufflers (muffler A: a one-chamber *HR* element and a one-chamber simple expansion element; muffler B; a one-chamber *HR* element and a one-chamber tube-extended element; muffler C; a one-chamber *HR* element and a one-chamber dissipative element).
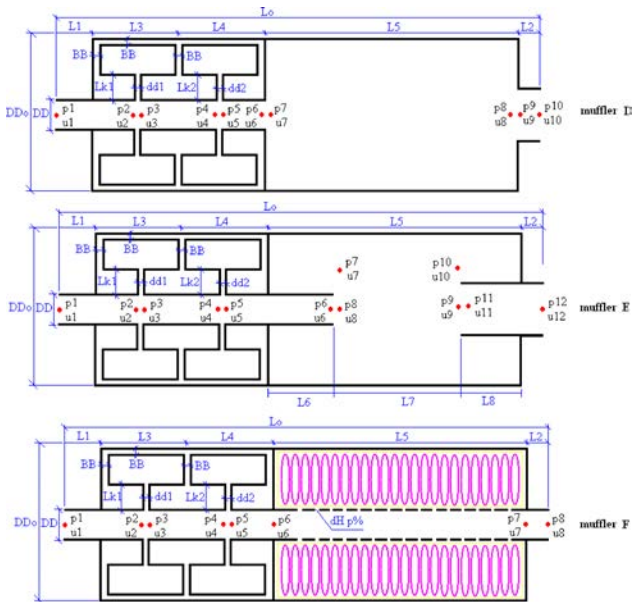

Fig. 3. The dimension and acoustical nodes for three kinds of two-chamber Helmholtz mufflers (muffler D; a two-chamber *HR* element and a one-chamber simple expansion element; muffler E; a two-chamber *HR* element and a one-chamber tube-extended element; muffler F; a two-chamber *HR* element and a one-chamber dissipative element).

adopted in dealing with a broadband noise hybridized with two tones (130 Hz and 235 Hz). The detailed mathematical derivation of various muffler systems is presented below.

2.1. Muffler A (a one-chamber HR element and a one-chamber simple expansion element)

As derived in previous work (CHIU, CHANG, 2008a; 2008b; CHIU, 2008; 2009; 2010a; 2010b; 2010c) and Appendix A, individual transfer matrixes with respect to straight ducts, an *HR* element, a sudden expanded duct, a sudden contracted duct, and a dissipative duct are described as follows:

$$\begin{pmatrix} p_1 \\ \rho_o c_o u_1 \end{pmatrix} = ff_1(L_1, L_3) \begin{bmatrix} TS1, 1_{1,1} & TS1, 1_{1,2} \\ TS1, 1_{2,1} & TS1, 1_{2,2} \end{bmatrix} \begin{pmatrix} p_2 \\ \rho_o c_o u_2 \end{pmatrix}, (1)$$

$$\begin{pmatrix} p_2 \\ \rho_o c_o u_2 \end{pmatrix} = \begin{bmatrix} THR1, 2_{1,1} & THR1, 2_{1,2} \\ THR1, 2_{2,1} & THR1, 2_{2,2} \end{bmatrix} \begin{pmatrix} p_3 \\ \rho_o c_o u_3 \end{pmatrix}, \qquad (2)$$

$$\begin{pmatrix} p_3 \\ \rho_o c_o u_4 \end{pmatrix} = ff_2(L_3) \begin{bmatrix} TS1, 3_{1,1} & TS1, 3_{1,2} \\ TS1, 3_{2,1} & TS1, 3_{2,2} \end{bmatrix} \begin{pmatrix} p_4 \\ \rho_o c_o u_4 \end{pmatrix}, \qquad (3)$$

$$\begin{pmatrix} p_4 \\ \rho_o c_o u_4 \end{pmatrix} = \begin{bmatrix} TSE1, 4_{1,1} & TSE1, 4_{1,2} \\ TSE1, 4_{2,1} & TSE1, 4_{2,2} \end{bmatrix} \begin{pmatrix} p_5 \\ \rho_o c_o u_5 \end{pmatrix}, \qquad (4)$$

$$\begin{pmatrix} p_5 \\ \rho_o c_o u_5 \end{pmatrix} = ff_3(L_4) \begin{bmatrix} TS1, 5_{1,1} & TS1, 5_{1,2} \\ TS1, 5_{2,1} & TS1, 5_{2,2} \end{bmatrix} \begin{pmatrix} p_6 \\ \rho_o c_o u_6 \end{pmatrix}, \qquad (5)$$

$$\begin{pmatrix} p_6 \\ \rho_o c_o u_6 \end{pmatrix} = \begin{bmatrix} TSC1, 6_{1,1} & TSC1, 6_{1,2} \\ TSC1, 6_{2,1} & TSC1, 6_{2,2} \end{bmatrix} \begin{pmatrix} p_7 \\ \rho_o c_o u_7 \end{pmatrix}, \qquad (6)$$

$$\begin{pmatrix} p_7 \\ \rho_o c_o u_7 \end{pmatrix} = ff_4(L_2) \begin{bmatrix} TS1, 7_{1,1} & TS1, 7_{1,2} \\ TS1, 7_{2,1} & TS1, 7_{2,2} \end{bmatrix} \begin{pmatrix} p_8 \\ \rho_o c_o u_8 \end{pmatrix}. \qquad (7)$$

The total transfer matrix assembled by multiplication is simplified as

$$\left\{ \begin{matrix} p_1 \\ \rho_o c_o u_1 \end{matrix} \right\} = \prod_m [T_m(f)] \left\{ \begin{matrix} p_8 \\ \rho_o c_o u_8 \end{matrix} \right\}. \qquad (8)$$

The sound transmission loss (*STL*) of a muffler is defined as (MUNJAL, 1987)

$$STL_1(Q, f, RT_1^{*A}, RT_2^{*A}, RT_3^{*A}, RT_4^{*A})$$
$$= 20 \log \left(\frac{1}{2}(T_{11} + T_{12} + T_{21} + T_{22}) \right)$$
$$+ 10 \log \left(\frac{S_1}{S_8} \right). \qquad (9)$$

2.2. Muffler B (a one-chamber HR element and a one-chamber tube-extended element) (CHIU, 2010a; 2010b; 2010c)

Similarly, the sound transmission loss (STL) is

$$STL_2(Q, f, RT_1^{*B}, RT_2^{*B}, RT_3^{*B},$$
$$RT_4^{*B}, RT_5^{*B}, RT_6^{*B})$$
$$= 20\log\left(\frac{1}{2}\left(T_{11} + T_{12} + T_{21} + T_{22}\right)\right)$$
$$+ 10\log\left(\frac{S_1}{S_{10}}\right). \tag{10}$$

2.3. Muffler C (a one-chamber HR element and a one-chamber dissipative element) (CHIU, 2011a; 2011b; 2012)

Also, the sound transmission loss (STL) is

$$STL_3(Q, f, RT_1^{*C}, RT_2^{*C}, RT_3^{*C}, RT_4^{*C}, RT_5^{*C})$$
$$= 20\log\left(\frac{1}{2}\left(T_{11} + T_{12} + T_{21} + T_{22}\right)\right)$$
$$+ 10\log\left(\frac{S_1}{S_6}\right). \tag{11}$$

2.4. Muffler D (a two-chamber HR element and a one-chamber simple expansion element)

Likewise, the related sound transmission loss (STL) is

$$STL_4(Q, f, RT_1^{*D}, RT_2^{*D}, RT_3^{*D},$$
$$RT_4^{*D}, RT_5^{*D}, RT_6^{*D})$$
$$= 20\log\left(\frac{1}{2}\left(T_{11} + T_{12} + T_{21} + T_{22}\right)\right)$$
$$+ 10\log\left(\frac{S_1}{S_{10}}\right). \tag{12}$$

2.5. Muffler E (a two-chamber HR element and a one-chamber tube-extended element)

Equally, the sound transmission loss (STL) is

$$STL_5(Q, f, RT_1^{*E}, RT_2^{*E}, RT_3^{*E}, RT_4^{*E},$$
$$RT_5^{*E}, RT_6^{*E}, RT_7^{*E}, RT_8^{*E})$$
$$= 20\log\left(\frac{1}{2}\left(T_{11} + T_{12} + T_{21} + T_{22}\right)\right)$$
$$+ 10\log\left(\frac{S_1}{S_{12}}\right). \tag{13}$$

2.6. Muffler F (a two-chamber HR element and a one-chamber dissipative element)

Also, the sound transmission loss (STL) is

$$STL_6(Q, f, RT_1^{*F}, RT_2^{*F}, RT_3^{*F}, RT_4^{*F},$$
$$RT_5^{*F}, RT_6^{*F}, RT_7^{*F})$$
$$= 20\log\left(\frac{1}{2}\left(T_{11} + T_{12} + T_{21} + T_{22}\right)\right)$$
$$+ 10\log\left(\frac{S_1}{S_8}\right). \tag{14}$$

2.7. Overall sound power level

The overall SWL_T silenced by the muffler at the outlet is

$$SWL_T = 10\log_{10}\left(\sum_m 10^{(SWL(f_m) - STL(f_m))/10}\right), \tag{15}$$

where $SWL(fm)$ is the original SWL at the inlet of the muffler (or pipe outlet), and m is the index of the octave band frequency, $STL(fm)$ is the muffler's STL with respect to the relative octave band frequency.

2.8. Objective function

By using the formulas of Eqs. (9)–(15), the objective function used in the SA optimization with respect to each type of muffler was established. For muffler A, the objective function in minimizing overall SWL_T hybridized with one tone (f_1) is

$$OBJ_1 = SWL_1(Q, f_1, RT_1^{*A}, RT_2^{*A}, RT_3^{*A}, RT_4^{*A}). \tag{16}$$

For muffler B, the objective function in minimizing overall SWL_T hybridized with one tone (f_1) is

$$OBJ_2 = SWL_2(Q, f_1, RT_1^{*B}, RT_2^{*B}, RT_3^{*B},$$
$$RT_4^{*B}, RT_5^{*B}, RT_6^{*B}). \tag{17}$$

For muffler C, the objective function in minimizing overall SWL_T hybridized with one tone (f_1) is

$$OBJ_3 = SWL_3(Q, f, RT_1^{*C}, RT_2^{*C}, RT_3^{*C},$$
$$RT_4^{*C}, RT_5^{*C}). \tag{18}$$

For muffler D, the objective function in minimizing overall SWL_T hybridized with two tones (f_1 and f_2) is

$$OBJ_4 = SWL_4(Q, f_1, f_2, RT_1^{*D}, RT_2^{*D}, RT_3^{*D},$$
$$RT_4^{*D}, RT_5^{*D}, RT_6^{*D}). \tag{19}$$

For muffler E, the objective function in minimizing overall SWL_T hybridized with two tones (f_1 and f_2) is

$$OBJ_5 = SWL_5(Q, f_1, f_2, RT_1^{*E}, RT_2^{*E}, RT_3^{*E}, RT_4^{*E},$$
$$RT_5^{*E}, RT_6^{*E}, RT_7^{*E}, RT_8^{*E}). \tag{20}$$

For muffler F, the objective function in minimizing overall SWL_T hybridized with two tones (f_1 and f_2) is

$$OBJ_6 = SWL_6(Q, f_1, f_2, RT_1^{*F}, RT_2^{*F}, RT_3^{*F},$$
$$RT_4^{*F}, RT_5^{*F}, RT_6^{*F}, RT_7^{*F}). \tag{21}$$

3. Model check

Before performing the *SA* optimal simulation on mufflers, an accuracy check of the mathematical model on the *HR* element is performed using the experimental data from SELAMET *et al.* (2005). As depicted in Fig. 4, the performance curve with respect to the theoretical and experimental data is relatively accurate and in agreement. Therefore, the proposed fundamental mathematical model with the *HR* element is acceptable. Consequently, the model linked with the numerical method is applied to the shape optimization in the following section.
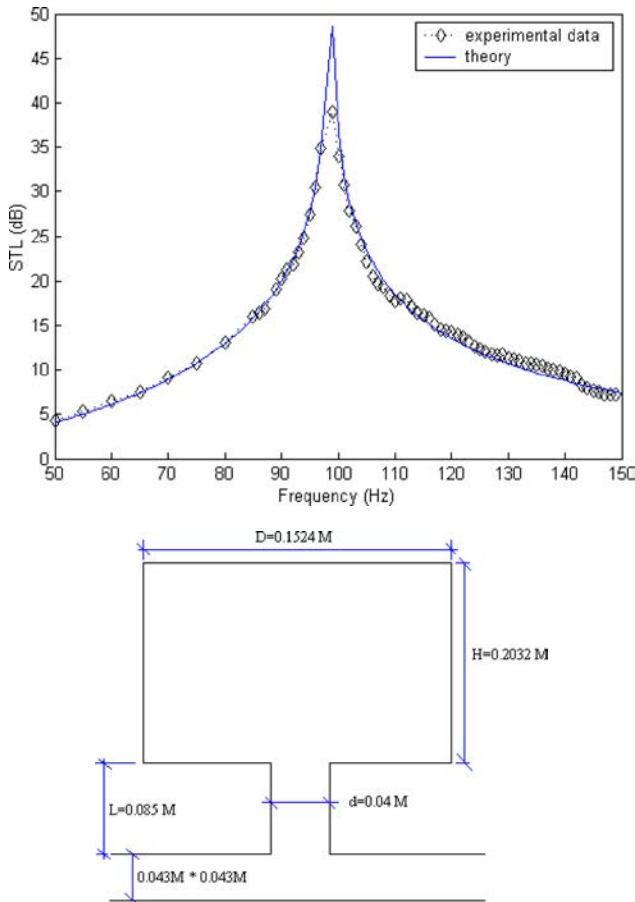

Fig. 4. Performance of a single-chamber Helmholtz muffler without the mean flow [experimental data is from SELAMET *et al.* (2005)].

4. Case studies

In this paper, a machine room within a constrained space is shown in Fig. 1. As shown in Fig. 1, the available space for a muffler is 0.5 m in width, 0.5 m in height, and 1.2 m in length. In Case I, the broadband noise is hybridized with one tone (130 Hz). In dealing with the broadband mixed with a one-tone noise, three kinds of two-chamber mufflers (muffler A: a one-chamber *HR* element and a one-chamber simple expansion element; muffler B: a one-chamber *HR* element and a one-chamber tube-extended element; muffler C: a one-chamber *HR* element and a one-chamber dissipative element) shown in Fig. 2 are proposed. Moreover, in Case II, the broadband noise is hybridized with two tones (130 Hz and 235 Hz). In dealing with the broadband mixed with a two-tone noise, three kinds of three-chamber mufflers (muffler D: a two-chamber *HR* element and a one-chamber simple expansion element; muffler E: a two-chamber *HR* element and a one-chamber tube-extended element; muffler F: a two-chamber *HR* element and a one-chamber dissipative element) shown in Fig. 3 are proposed. The related sound power level inside the muffler inlet for Case I and Case II are shown in Table 1. The ranges of the parameters of the mufflers are listed in Table 2. The flowing resistance (σ_{fr}) of the absorbing material filled in the dissipative element is assumed to be 22000 rayls/m. In the existing venting system, the flow rate (Q) is given as 0.01 (m³/s).

Table 1. The original Sound Power Level in Case I and Case II.

Case I		Case II	
Frequency [Hz]	*SWL* [dB]	Frequency [Hz]	*SWL* [dB]
50	76	50	78
60	77	60	79
70	79	70	80
80	81	80	83
90	87	90	89
100	93	100	95
110	105	110	107
125	126	125	128
130	139	130	139
140	125	140	129
150	116	200	112
160	108	235	135
250	95	250	124
500	99	500	91
1000	100	1000	95
2000	104	2000	104
Overal [dB]	139.4	Overall	141.1

Table 2. The ranges of parameters for mufflers A–F.

Item	ranges of parameters
Muffler A	$RT_1^{*A} = [0.2, 0.4]$; $RT_2^{*A} = [0.003, 0.02]$; $RT_3^{*A} = [0.02, 0.05]$; $RT_4^{*A} = [0.2, 0.4]$
Muffler B	$RT_1^{*B} = [0.2, 0.4]$; $RT_2^{*B} = [0.003, 0.02]$; $RT_3^{*B} = [0.02, 0.05]$; $RT_4^{*B} = [0.2, 0.4]$; $RT_5^{*B} = [0.2, 0.4]$; $RT_6^{*B} = [0.2, 0.4]$
Muffler C	$RT_1^{*C} = [0.2, 0.4]$; $RT_2^{*C} = [0.003, 0.02]$; $RT_3^{*C} = [0.02, 0.05]$; $RT_4^{*C} = [0.00175, 0.007]$; $RT_5^{*C} = [0.03, 0.1]$
Muffler D	$RT_1^{*D} = [0.2, 0.4]$; $RT_2^{*D} = [0.003, 0.02]$; $RT_3^{*D} = [0.003, 0.02]$; $RT_4^{*D} = [0.02, 0.05]$; $RT_5^{*D} = [0.02, 0.05]$; $RT_6^{*D} = [0.2, 0.4]$
Muffler E	$RT_1^{*E} = [0.2, 0.4]$; $RT_2^{*E} = [0.003, 0.02]$; $RT_3^{*E} = [0.003, 0.02]$; $RT_4^{*E} = [0.02, 0.05]$; $RT_5^{*E} = [0.02, 0.05]$; $RT_6^{*E} = [0.2, 0.4]$; $RT_7^{*E} = [0.2, 0.4]$; $RT_8^{*E} = [0.2, 0.4]$
Muffler F	$RT_1^{*F} = [0.2, 0.4]$; $RT_2^{*F} = [0.003, 0.02]$; $RT_3^{*F} = [0.003, 0.02]$; $RT_4^{*F} = [0.02, 0.05]$; $RT_5^{*F} = [0.02, 0.05]$; $RT_6^{*F} = [0.00175, 0.007]$; $RT_7^{*F} = [0.03, 0.1]$

5. Simulated annealing

The fundamental concept of simulated annealing (SA), a local search process which imitates the softness process (annealing) of metal and is started by generating a random initial solution, was first introduced by Metropolis *et al.* (1953) and subsequently developed by Kirkpatrick *et al.* (1983). The SA scheme is a variation of the hill-climbing algorithm where all downhill movements are accepted for the decrement of the system's energy. However, in order to escape the local optimum, solutions that are inferior (uphill moves) to the current one are allow. Here, the optimal process is dominated by two primary parameters – kk and iter; for next steps of optimizing calculation of the cases considered, the SA procedure described in our previous paper has been applied (Chiu, 2008; 2009; 2010a; 2010b; 2011a; Chiu, Chang, 2008b) where kk is the cooling rate and iter is the maximal iteration. The SA process is repeated until the predetermined number (iter) of the outer loop is reached.

6. Results and discussion

6.1. Results

The accuracy of the SA optimization depends on the cooling rate (kk) and the number of iterations (iter). To achieve a good optimization, the range of both the cooling rate and the number of iterations are set as $kk = [0.91, 0.93, 0.95, 0.97, 0.99]$ and iter $= [50, 100, 500, 1000]$.

An optimization for muffler B in reducing the broadband noise in Case I by varying the kk and the iter has been approached and shown in Table 3. Using Table 3, the optimal STL curves with respect to various SA parameters (kk and iter) are plotted and depicted in Figs. 5–6. As indicated in Table 3 and Figs. 5–6, the best result occurs at the eighth set when $kk = 0.99$ and iter $= 1000$ are applied. Applying the above best SA parameter set in the optimization of muffler A and muffler C, the resultant design parameters and minimized SWLs have been obtained and shown in Table 4. Using the optimal design data of mufflers A–C in Table 4, the optimal STL curves with respect to the original SWL curve are plotted and depicted in Fig. 7.

Table 3. Optimal design data with respect to various SA parameters (kk, iter) for muffler B.

Item	SA parameters		Results						
1	kk	iter	RT_1^{*B}	RT_2^{*B}	RT_3^{*B}	RT_4^{*B}	RT_5^{*B}	RT_6^{*B}	SWL_2 [dB]
	0.91	50	0.3402	0.01492	0.04104	0.3402	0.3402	0.3402	106.3
2	kk	iter	RT_1^{*B}	RT_2^{*B}	RT_3^{*B}	RT_4^{*B}	RT_5^{*B}	RT_6^{*B}	SWL_2 [dB]
	0.93	50	0.2541	0.0076	0.02812	0.2541	0.2541	0.2541	101.3
3	kk	iter	RT_1^{*B}	RT_2^{*B}	RT_3^{*B}	RT_4^{*B}	RT_5^{*B}	RT_6^{*B}	SWL_2 [dB]
	0.95	50	0.2630	0.00835	0.02945	0.2630	0.2630	0.2630	96.3
4	kk	iter	RT_1^{*B}	RT_2^{*B}	RT_3^{*B}	RT_4^{*B}	RT_5^{*B}	RT_6^{*B}	SWL_2 [dB]
	0.97	50	0.2577	0.0079	0.0286	0.2577	0.2577	0.2577	95.3
5	kk	iter	RT_1^{*B}	RT_2^{*B}	RT_3^{*B}	RT_4^{*B}	RT_5^{*B}	RT_6^{*B}	SWL_2 [dB]
	0.99	50	0.2846	0.01019	0.03269	0.2846	0.2846	0.2846	91.9
6	kk	iter	RT_1^{*B}	RT_2^{*B}	RT_3^{*B}	RT_4^{*B}	RT_5^{*B}	RT_6^{*B}	SWL_2 [dB]
	0.99	100	0.2089	0.00375	0.02133	0.2089	0.2089	0.2089	87.0
7	kk	iter	RT_1^{*B}	RT_2^{*B}	RT_3^{*B}	RT_4^{*B}	RT_5^{*B}	RT_6^{*B}	SWL_2 [dB]
	0.99	500	0.2114	0.00397	0.02171	0.2114	0.2114	0.2114	85.8
8	kk	iter	RT_1^{*B}	RT_2^{*B}	RT_3^{*B}	RT_4^{*B}	RT_5^{*B}	RT_6^{*B}	SWL_2 [dB]
	0.99	1000	0.2157	0.00433	0.02235	0.2157	0.2157	0.2157	85.0

Table 4. Optimal design data with respect to various mufflers ($kk = 0.99$; iter $= 1000$).

Item	Results								
Muffler A	RT_1^{*A}	RT_2^{*A}	RT_3^{*A}	RT_4^{*A}					SWL_1 [dB]
	0.2251	0.00513	0.02376	0.2251					92.9
Muffler B	RT_1^{*B}	RT_2^{*B}	RT_3^{*B}	RT_4^{*B}	RT_5^{*B}	RT_6^{*B}			SWL_2 [dB]
	0.2157	0.00433	0.02235	0.2157	0.2157	0.2157			85.0
Muffler C	RT_1^{*C}	RT_2^{*C}	RT_3^{*C}	RT_4^{*C}	RT_5^{*C}				SWL_3 [dB]
	0.3031	0.01177	0.03547	0.004457	0.0661				82.5
Muffler D	RT_1^{*D}	RT_2^{*D}	RT_3^{*D}	RT_4^{*D}	RT_5^{*D}	RT_6^{*D}			SWL_4 [dB]
	0.2680	0.00878	0.00878	0.0302	0.0302	0.2680			91.1
Muffler E	RT_1^{*E}	RT_2^{*E}	RT_3^{*E}	RT_4^{*E}	RT_5^{*E}	RT_6^{*E}	RT_7^{*E}	RT_8^{*E}	SWL_5 [dB]
	0.2143	0.00421	0.00421	0.02215	0.02215	0.2143	0.2143	0.2143	80.4
Muffler F	RT_1^{*F}	RT_2^{*F}	RT_3^{*F}	RT_4^{*F}	RT_5^{*F}	RT_6^{*F}	RT_7^{*F}		SWL_6 [dB]
	0.2629	0.00834	0.00834	0.02943	0.02943	0.0034	0.05201		71.4

Note:

Muffler A – $RT_1^{*A} = DD/D_o$; $RT_2^{*A} = dd_1$; $RT_3^{*A} = Lk_1$; $RT_4^{*A} = DD_1/D_o$

Muffler B – $RT_1^{*B} = DD/D_o$; $RT_2^{*B} = dd_1$; $RT_3^{*B} = Lk_1$; $RT_4^{*B} = DD_1/D_o$; $RT_5^{*B} = L_5/L_4$; $RT_6^{*B} = L_7/L_4$

Muffler C – $RT_1^{*C} = DD/D_o$; $RT_2^{*C} = dd_1$; $RT_3^{*C} = Lk_1$; $RT_4^{*C} = dH$; $RT_5^{*C} = p\%$

Muffler D – $RT_1^{*D} = DD/D_o$; $RT_2^{*D} = dd_1$; $RT_3^{*D} = dd_2$; $RT_4^{*D} = Lk_1$; $RT_5^{*D} = Lk_2$; $RT_6^{*D} = DD_1/D_o$

Muffler E – $RT_1^{*E} = DD/D_o$; $RT_2^{*E} = dd_1$; $RT_3^{*E} = dd_2$; $RT_4^{*E} = Lk_1$; $RT_5^{*E} = Lk_2$; $RT_6^{*E} = DD_1/D_o$; $RT_7^{*E} = L_6/L_5$; $RT_8^{*E} = L_8/L_5$

Muffler F – $RT_1^{*F} = DD/D_o$; $RT_2^{*F} = dd_1$; $RT_3^{*F} = dd_2$; $RT_4^{*F} = Lk_1$; $RT_5^{*F} = Lk_2$; $RT_6^{*F} = dH$; $RT_7^{*F} = p\%$
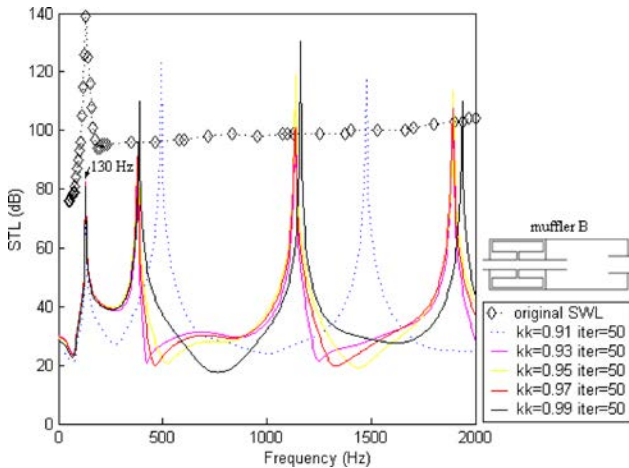

Fig. 5. Comparison of the original SWL with respect to the STL at various kk parameters for muffler B (iter $= 50$).
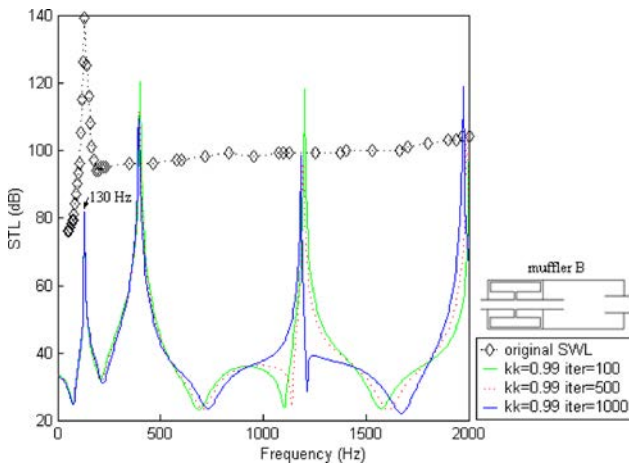

Fig. 6. Comparison of the original SWL with respect to the STL at various iter parameters for muffler B ($kk = 0.99$).
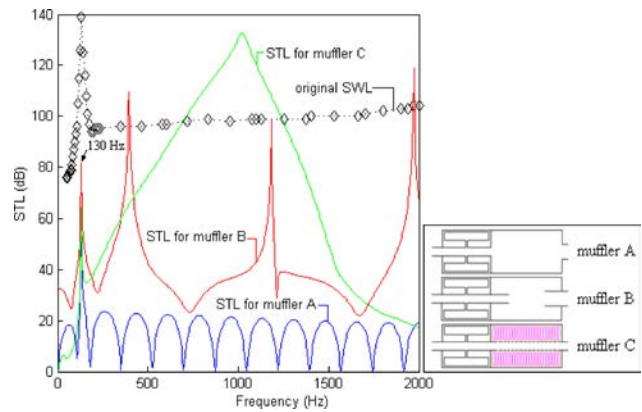

Fig. 7. Comparison of the original SWL (hybridized with a pure tone – 130 Hz) with respect to the STL at various mufflers [muffler A; a one-chamber HR element and a one-chamber simple expansion element; muffler B; a one-chamber HR element and a one-chamber tube-extended element; muffler C; a one-chamber HR element and a one-chamber dissipative element].

Similarly, using the same SA parameter set in Case II, the optimization for mufflers D–F has been approached and shown in Table 4. Using the optimal design data of mufflers D–F in Table 4, the optimal STL curves with respect to the original SWL curve are plotted and depicted in Fig. 8.

6.2. Discussion

As described in Subsec. 6.1, in seeking a better STL with three kinds of mufflers (mufflers A–C) in Case I, a shape optimization process in conjunction
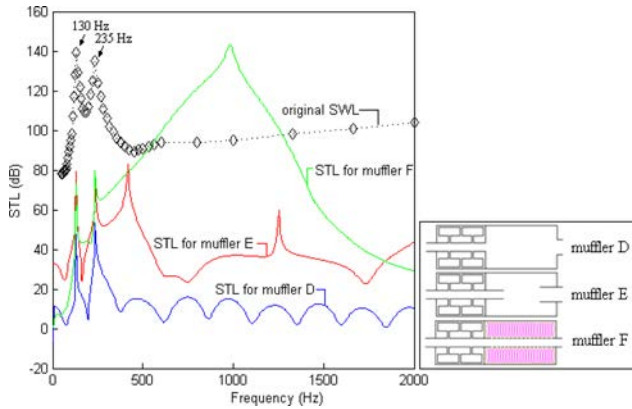
Fig. 8. Comparison of the original *SWL* (hybridized with two pure tone – 130 Hz and 235 Hz) with respect to the *STL* at various mufflers [muffler D; a two-chamber *HR* element and a one-chamber simple expansion element; muffler E; a two-chamber *HR* element and a one-chamber tube-extended element; muffler F; a two-chamber *HR* element and a one-chamber dissipative element].

with the *SA* optimizer is performed. As indicated in Table 1 and Table 4, the *SWL* at the venting outlet will be reduced from 139.4 dB to 92.9 when muffler A is added. The *SWL* at the venting outlet will be reduced from 139.4 dB to 85.0 when muffler B is adopted. Similarly, the *SWL* at the venting outlet will be reduced from 139.4 dB to 82.5 when muffler C is used. As indicated in Fig. 7, it is obvious that the peak value at a pure tone of 130 Hz has been reduced by using the *HR* element in mufflers A–C. Moreover, considering the overall acoustical effect, muffler C, having a one-chamber *HR* equipped with a dissipative element, is superior to muffler A (a one-chamber *HR* equipped with a one-chamber simple expansion element) and muffler B (a one-chamber *HR* equipped with a one-chamber tube-extended element).

Similarly, a shape optimization process in Case II is performed. The results shown in Table 4 indicate that the *SWL* at the venting outlet will be reduced from 141.1 dB to 91.1 when muffler D is added. The *SWL* at the venting outlet will be reduced from 141.1 dB to 80.4 when muffler E is adopted. Also, the *SWL* at the venting outlet will be reduced from 141.1 dB to 71.4 when muffler F is used. As indicated in Fig. 8, it is obvious that the peak values at the pure tones of 130 Hz and 235 Hz have been fully eliminated by using the two *HR* elements in mufflers D∼F. Moreover, considering the overall acoustical effect, muffler F, having a two-chamber *HR* equipped with a dissipative element, is superior to muffler D (a two-chamber *HR* equipped with a one-chamber simple expansion element) and muffler E (a two-chamber *HR* equipped with a one-chamber tube-extended element).

7. Conclusions

It has been shown that hybrid *HR* mufflers used in dealing with a broadband noise hybridized with multiple tones can be easily and efficiently optimized within a limited space by using a four-pole transfer matrix as well as a *SA* optimizer. Two kinds of *SA* parameters (*kk*, iter) play essential roles in the solution's accuracy during the *SA* optimization. As indicated in Figs. 5–6, the tuning ability established by adjusting the design parameters of muffler B is reliable.

As investigated in Case I in Sec. 6 and indicated in Fig. 7, the peak value (at 130 Hz) of the *SWL* at the venting outlet of the machine room can be eliminated by using the one-chamber *HR* in mufflers A–C. Considering the overall acoustical effect, the overall silenced *SWL* with respect to mufflers A–C reached 92.9 dB, 85.0 dB, and 82.5 dB. It is obvious that muffler C with a noise reduction of 54.9 dB is superior to the other mufflers. Moreover, for the numerical approach in Case II, Fig. 8 reveals that the peak values (at 130 Hz and 235 Hz) of the *SWL* at the venting outlet of the machine room also can be eliminated by using two chambers of the *HR* equipped in mufflers D–F. Similarly, the overall silenced *SWL* with respect to mufflers D–F reached 91.1 dB, 80.4 dB, and 71.4 dB. It is obvious that muffler F with a noise reduction of 69.7 dB is superior to the other mufflers. Consequently, the approach used for the optimal noise elimination in the broadband noise hybridized with multiple tones proposed in this study within a limited space is quite important and easily achieved.

Appendix A. Transfer matrix of a Helmholtz Resonator Muffler

As indicated in Fig. 9, the one-array Helmholtz Resonator (*HR*) muffler has one chamber in a sectional direction. Assuming that the characteristic length of the *HR* element is smaller than the acoustical wave, the neck of the resonator can be regarded as a lumped mass. The air compression is analogous to a spring during the adiabatic resonating process. Considering the acoustical end correction, the factors (ℓ_1 and ℓ_2) of the end correction with the flange are (LORD, RAYLEIGH, 1945)
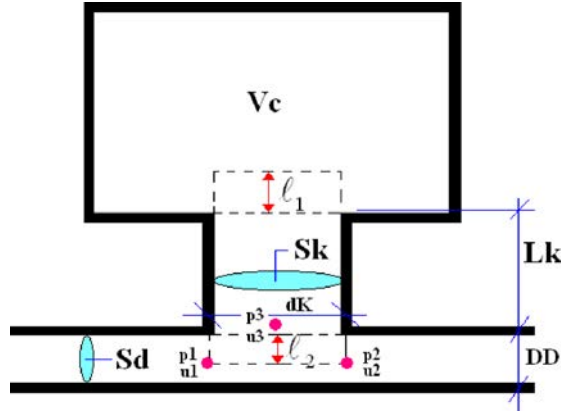
$$\ell_1 = \ell_2 = \frac{8r_k}{3\pi} = 0.849r_k. \qquad (22)$$

For a simplified mathematical model of the *HR* element, the resonant frequency (f_{res}) is

$$f_{\text{res}} = \frac{c_o}{2\pi}\sqrt{\frac{S_k}{V_c(L_k + \ell_T)}}, \qquad (23)$$

where c_o is the sound speed, S_k is the section area of the resonating neck, L_k is the length of the resonating
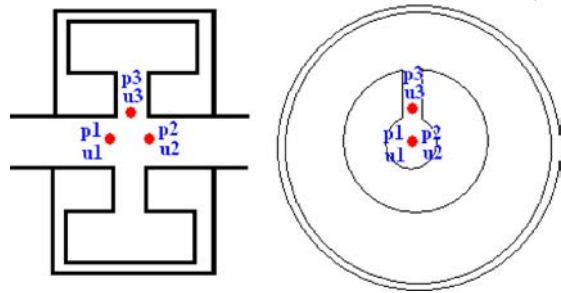
a) element with a symbol

b) section view

Fig. 9. A one-chamber Helmholtz resonator (HR) muffler.

neck, V_c is the volume of the resonator, ℓ_T is the total end correction.

The acoustical impedance (Z_r) is expressed as

$$Z_r = R_{\text{res}} + j\omega L_{\text{res}} + \frac{1}{j\omega C_{\text{res}}}. \tag{24}$$

According to MUNJAIL (1987), the acoustic resistance for a resonator with a radius r_k at the neck is

$$R_{\text{res}} = Y_o\left\{ \frac{(2k_o r_k)^2}{2\cdot4} - \frac{(2k_o r_k)^4}{2\cdot4^2\cdot6} + \frac{(2k_o r_k)^6}{2\cdot4^2\cdot6^2\cdot8} - ... \right\}. \tag{25}$$

The sound wave can be regarded as a plane wave by neglecting the high order term when $k_o r_k < 0.5$.

The acoustic resistance is simplified as

$$R_{\text{res}} = 2\frac{\rho_o\omega^2}{2\pi c_o}. \tag{26}$$

The property of the acoustic pressure (p) and the acoustic mass velocity (ν) for nodes 1–3 is

$$p_1 = p_3, \quad p_2 = p_3, \quad \nu_3 = \nu_1 + \nu_2, \tag{27}$$

where

$$\begin{aligned} \nu_1 &= \rho_o c_o S_d u_1, \\ \nu_2 &= \rho_o c_o S_d u_2, \\ \nu_3 &= \rho_o c_o S_k u_3. \end{aligned} \tag{28}$$

Substituting Eq. (28) for Eq. (27) yields

$$\begin{aligned} p_3 &= p_1, \\ \rho_o c_o u_3 &= \rho_o c_o u_1 + \frac{c_o}{S_d Z_r} p_1. \end{aligned} \tag{29}$$

Rearranging Eq. (29) in matrix form yields

$$\begin{pmatrix} p_3 \\ \rho_o c_o u_3 \end{pmatrix} = \begin{bmatrix} 1 & 0 \\ \dfrac{c_o}{S_d Z_r} & 1 \end{bmatrix} \begin{pmatrix} p_1 \\ \rho_o c_o u_1 \end{pmatrix}. \tag{30}$$

The acoustic resistance R_{res} is ignored as zero when the resonation occurred. The acoustical impedance (Z_r) is simplified as

$$Z_r = j\omega L_{\text{res}} + \frac{1}{j\omega C_{\text{res}}}. \tag{31}$$

References

1. ALLEY B.C., DUFRESNE R.M., KANJI N., REESAL M.R. (1989), *Costs of workers' compensation claims for hearing loss*, Journal of Occupational Medicine, **31**, 134–138.

2. ALSTER M. (1972), *Improved calculation of resonant frequencies of Helmholtz resonators*, J. Sound Vib., **24**, 63–85.

3. CHANAUD R.C. (1994), *Effects of geometry on the resonance frequency of Helmholtz resonators*, J. Sound Vib., **178**, 337–348.

4. CHANAUD R.C. (1997), *Effects of geometry on the resonance frequency of Helmholtz resonators*, Part II., J. Sound Vib., **204**, 5, 829–834.

5. CHEREMISINOFF P.N., CHEREMISINOFF P.P. (1977), *Industrial noise control handbook*, Ann Arbor Science, Michigan.

6. CHIU M.C. (2008), *Shape optimization of double-chamber side mufflers with extended tube by using four-pole matrix and simulated annealing method*, J. of Mechanics, **24**, 31–43.

7. CHIU M.C., CHANG Y.C. (2008), *Numerical studies on venting system with multi-chamber perforated mufflers by GA optimization*, Applied Acoustics, **69**, 11, 1017–1037.

8. CHIU M.C., CHANG Y.C. (2008), *Shape optimization of multi-chamber cross-flow mufflers by SA optimization*, J. Sound Vib., **312**, 526–550.

9. CHIU M.C. (2009), *SA optimization on multi-chamber mufflers hybridized with perforated plug-inlet under space constraints*, Archives of Acoustics, **34**, 3, 305–343.

10. CHIU M.C. (2010a), *Numerical assessment of reverse-flow mufflers using a simulated annealing method*, The Canadian Society for Mechanical Engineering (CSME) Transactions, **34**, 1, 17–35.

11. CHIU M.C. (2010b), *Optimal design of multi-chamber mufflers hybridized with perforated intruding inlets and resonated tube using simulated annealing*, ASME J. of Vibration and Acoustics, **132**, 1–10.

12. CHIU M.C. (2010c), *Shape optimization of multi-chamber mufflers with plug-inlet tube on a venting process by genetic algorithms*, Applied Acoustics, **71**, 495–505.

13. CHIU M.C. (2011a), *Numerical assessment of hybrid mufflers on a venting system within a limited back pressure and space using simulated annealing*, J. of Low Frequency Noise, Vibration and Active Control, 30, 4, 247–275.

14. CHIU M.C. (2011b), *Optimization design of hybrid mufflers on broadband frequencies using the genetic algorithm*, Archives of Acoustics, **36**, 4, 795–822.

15. CHIU M.C. (2012), *Genetic algorithm optimization on a venting system with three-chamber hybrid mufflers within a constrained back pressure and space*, ASME J. of Vibration and Acoustics, **134**, 021005, 1–11.

16. CUMMINGS A. (1992), *The effects of a resonator array on the sound field in a cavity*, J. Sound Vib., **154**, 1, 25–44.

17. DICKEY N.S., SELAMET A. (1996), *Helmholtz resonators: one-dimensional limit for small cavity length-to-diameter ratios*, J. Sound Vib., **195**, 512–517.

18. DORIA A. (1995), *Control of acoustic vibrations of an enclosure by means of multiple resonators*, J. Sound Vib., **181**, 4, 673–685.

19. FAHY F.J., SCHOFIELD C. (1980), *A note on the interaction between a Helmholtz resonator and an acoustic mode of an enclosure*, J. Sound Vib., **72**, 3, 365–378.

20. HELMHOLTZ H.V., VON DEN L. (1877), *Tonempfindungen*, Vieweg Verlag, Braunschweig.

21. HSIEH J.L. (2003), *Attenuation of motorcycle intake Noise*, Feng Chia University, Taiwan.

22. INGARD U. (1953), *On the theory and design of acoustic resonators*, J. Acoust. Soc. Am., **25**, 6, 1037–1061.

23. KIRKPATRICK S., GELATT C.D., VECCHI M.P. (1983), *Optimization by simulated annealing*, Science, **220**, 671–680.

24. LEUG P. (1936), *Process of silencing sound oscillations*, U. S. Patent, 2 043 416.

25. LI D., CHENG L. (2007), *Acoustically coupled model of an enclosure and Helmholtz resonator Array*, J. Sound Vib., **305**, 272–288.

26. LORD J.W., RAYLEIGH S. (1945), *The theory of sound*, Dover Publicaions, Inc., New York.

27. METROPOLIS A., ROSENBLUTH W., ROSENBLUTH M.N., TELLER H., TELLER E. (1953), *Equation of static calculations by fast computing machines*, The Journal of Chemical Physics, **21**, 1087–1092.

28. MUNJAL M.L. (1987), *Acoustics of ducts and mufflers with application to exhaust and ventilation system design*, John Wiley & Sons, New York.

29. OLSEN H.F., MAY E.G. (1953), *Electronic sound absorber*, J. Acoust. Soc. Am., **25**, 1130–1136.

30. RAYLEIGH L. (1896), *Theory of sound II*, Macmillan, London.

31. SELAMET J., XU M.B., LEE I.J. (2005), *Helmholtz resonator lined with absorbing material*, J. Acoust. Soc. Am., **117**, 2, 725–733.

32. SUGIMOTO N. (1992), *Propagation of nonlinear acoustic waves in a tunnel with an array of Helmholtz resonators*, J. Fluid Mech., **244**, 55–78.

33. SUGIMOTO N., HORIOKA T. (1995), *Dispersion characteristics of sound waves in a tunnel with an array of Helmholtz resonators*, J. Acoust. Soc. Am., **97**, 1446–1459.

34. TANG S.K. (2005), *On Helmholtz resonators with tapered necks*, J. Sound Vib., 279, 1085–1096.